STATE OF OREGON
DEPARTMENT OF GEOLOGY AND MINERAL INDUSTRIES
Suite 965, 800 NE Oregon St., #28
Portland, Oregon 97232

Interpretive Map Series

IMS-14

Relative Earthquake Hazard Map of the Eugene-Springfield Metropolitan Area, Lane County, Oregon

By
Gerald L. Black, Zhenming Wang, Thomas J. Wiley, and Yumei Wang,
Oregon Department of Geology and Mineral Industries
and
David K. Keefer,
U.S. Geological Survey

2000

Text

IMPORTANT NOTICE FOR INTERPRETIVE SERIES MAP IMS-14

This map depicts earthquake hazard zones that are based on limited geologic and geophysical data, as described in the text. **The map is not a substitute for site-specific investigations by qualified practitioners.** At any point in the map area, site-specific data may give results that differ from those shown on the map. Some appropriate uses for the map are discussed in the text. For a complete understanding of the earthquake hazard, consultation of the following Department publication is also recommended: Madin, I.P., and Mabey, M.A., 1996, *Earthquake hazard maps for Oregon*: Oregon Department of Geology and Mineral Industries Geological Map Series GMS-100.

Interpretive Map Series

IMS-14

Relative Earthquake Hazard Map of the Eugene-Springfield Metropolitan Area, Lane County, Oregon

By

Gerald L. Black, Zhenming Wang, Thomas J. Wiley, and Yumei Wang,
Oregon Department of Geology and Mineral Industries
and
David K. Keefer,
U.S. Geological Survey

ABSTRACT

This *Relative Earthquake Hazard Map of the Eugene-Springfield Metropolitan Area* depicts the relative risk of earthquake damage that results from local geologic conditions. On a neighborhood-to-neighborhood scale, local geologic conditions contribute as much as, or more than, any other factor to the hazard portion of a risk assessment. Showing in relative terms on a single map the hazard contribution of different earthquake-related hazards allows a nongeologic and nonengineering audience to work more effectively toward reducing the risk to life and property through planning, policy, and mitigation measures. The composite hazard map was developed by combining single hazard maps for ground motion amplification and slope instability. The single component maps were developed to show geographic patterns of stronger earthquake effects for two likely earthquake sources. Zones that are expected to have the most pronounced damage in any moderate or larger earthquake are shown on the map as having the greatest hazard.

INTRODUCTION

Since the late 1980s, there has been a significant increase in the understanding of earthquake hazards in the Pacific Northwest. It is now known that damaging earthquakes much larger than those that have occurred in the historical past are possible (Atwater, 1987; Heaton and Hartzell, 1987; Weaver and Shedlock, 1989; Yelin and others, 1994). Mitigation measures are a cost-effective means to minimize the damage that might occur in a strong earthquake. These measures should be based on the best possible assessment of the extent and distribution of earthquake damage. Earthquake hazard maps are one way to prioritize mitigation efforts.

The amount of damage sustained by a building during a strong earthquake is difficult to predict and is a function of the size, type, duration, and location of the earthquake, the characteristics of the soils at the building site, and the characteristics of the structure. At present, scientists cannot accurately assess the location or size of future earthquakes. They can, however, predict the behavior of the soil column at any particular site.

These maps are an attempt to identify those areas within the Eugene-Springfield Metropolitan Plan Boundary that will suffer more damage, relative to other areas, during a damaging earthquake. The analysis is based on the behavior of the soils and does not depict the absolute earthquake hazard at any particular site. In order to understand how the soil behaves at one site relative to another, it is necessary to use specific design earthquakes for the analysis. For this study, the design earthquakes were a magnitude (M) 6.5 crustal earthquake at a focal distance of 10 km (~6 mi) and a M 8.5 subduction zone earthquake at a focal distance of 100 km (~60 mi). However, it is unlikely that any "real" earthquake will exactly match our design parameters. It is quite possible that, for any given earthquake, damage in even the highest relative hazard areas will be light. For instance, the earthquake might cause damage but be of lower magnitude or occur at a greater distance than our design earthquake. On the other hand, during an earthquake that is stronger or much closer than our design parameters, even the areas in the lowest relative hazard categories could experience severe damage. This serves to reemphasize that we do not know where future earthquakes will occur or how big they will be.

The assessment of soil behavior (and hence the relative earthquake hazard) is based on geologic mapping and specialized geophysical and geotechnical measurements. These measurements are combined with state-of-practice geotechnical analysis and Geographic Information System (GIS) methodology and tools to produce the final map. The result is a map that divides the map area into four relative hazard zones; ranked from the greatest hazard (Zone A) to the least hazard (Zone D). Because of the way the relative earthquake hazard is calculated, Zone A does not occur in the Eugene-Springfield area. The reason for this is discussed in the section titled "Relative earthquake hazard map".

Because the map exists as "layers" of digital GIS data, it can easily be combined with earthquake source information to produce earthquake damage scenarios. The map can also be combined with maps of earthquake probability to provide an assessment of the absolute level of hazard and an estimate of how often that level will occur. Finally, the map can also be easily combined with GIS data for land use planning.

Levson and others (1995) described several applications of relative earthquake hazard maps to land use and emergency planning. They include: (1) identification of areas with vulnerable lifeline systems; (2) planning of transportation and utility corridors; (3) setting priorities for seismic upgrades for structures such as schools, hospitals, and other public safety and essential facilities; (4) initial screening for new sites for essential facilities; (5) identification of areas requiring special study before development; (6) identifying high-hazard areas with restricted development; (7) property insurance; (8) assessment of risk for financing new projects; (9) providing information on site effects for the design of new structures; and (10) establishing more stringent design requirements where needed.

EARTHQUAKE HAZARD

Earthquakes from three different sources threaten communities in western Oregon (Figure 1). These sources are crustal, intraplate, and subduction zone earthquakes. The most common are *crustal earthquakes*, which occur in the North American plate above the subduction zone at relatively shallow depths of 10–20 km (6–12 mi) below the surface. The 1993 earthquake at Scotts Mills (M 5.6) (Madin and others, 1993) and the 1993 Klamath Falls main shocks (M 5.9 and M 6.0) (Wiley and others, 1993) were crustal earthquakes.

Deeper *intraplate earthquakes* occur within the remains of the ocean floor (the Juan de Fuca plate) subducted beneath North America. Intraplate earthquakes caused damage in the Puget Sound region in 1949 and again in 1965. This type of earthquake could occur directly beneath the Eugene-Springfield metropolitan area at depths of 40–60 km (25–37 mi).

Great *subduction zone earthquakes* occur around the world where the plates that make up the surface of the Earth collide. When the plates collide, one plate is shoved ("subducts") beneath the other, where it is reabsorbed into the mantle. This dipping interface between the two plates is the site of some of the most powerful earthquakes ever recorded, often having magnitudes of 8 to 9 on the moment magnitude scale. The 1960 Chilean (M 9.5) and the 1964 Great Alaska (M 9.2) earthquakes were subduction zone earthquakes (Kanamori, 1977). The Cascadia subduction zone, which lies off the Oregon and Washington coasts, has been recognized for many years. There have been no earthquakes on the Cascadia subduction zone during our short 200-year historical record. However, in the last several years, various studies have found widespread evidence that very large earthquakes have occurred repeatedly in the past, most recently about 300 years ago, in January 1700 (e.g., Atwater, 1987). Best available evidence indicates that these earthquakes occur, on average, every 500–540 years; observed intervals between individual events range from about 200 to about 1,000 years (Atwater and Hemphill-Haley, 1997). There is every reason to believe that they will continue to occur in the future.

All three types of earthquakes threaten the Eugene-Springfield area. However, because the strength of shaking decreases with increasing distance from the earthquake source, the most severe shaking will result from either shallow crustal earthquakes or great subduction zone earthquakes (Mabey and others, 1993).

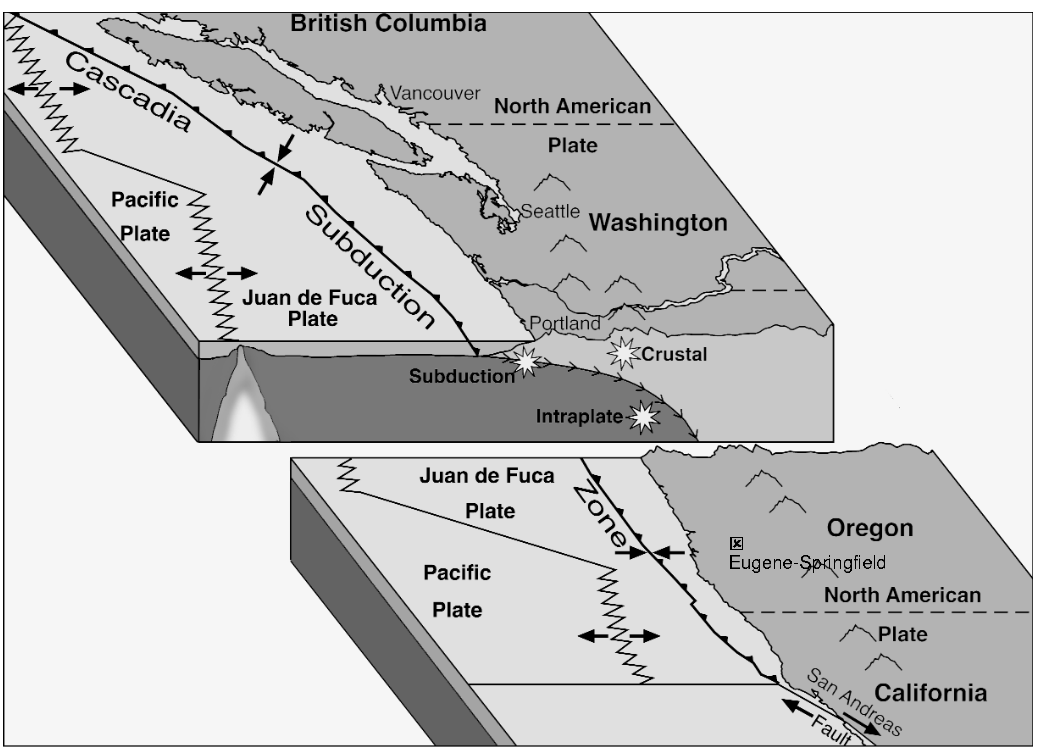

Figure 1. Schematic showing the regional plate tectonics setting and the three types of earthquake sources in the Pacific Northwest: subduction, intraplate, and crustal earthquakes.

EARTHQUAKE EFFECTS

Damaging earthquakes do affect the cities and towns of western Oregon, as was demonstrated by the Scotts Mills earthquake (M 5.6) in 1993 (Madin and others, 1993). The Eugene-Springfield area is no exception. Although we cannot predict when the next damaging earthquake will strike, where it will occur, or how large it will be, we can evaluate the influence of site geology on potential earthquake damage. This evaluation can occur while the exact sources of earthquake shaking are still being studied.

The most severe damage done by an earthquake commonly occurs in areas that experience one or more of the following phenomena: (1) amplification of ground shaking in a "soft" soil column; (2) liquefaction of water-saturated sand, silt, or gravel, creating areas of "quicksand"; and (3) landslides triggered by shaking. These effects can be evaluated before the earthquake occurs, if data are available on the thickness and nature of the geologic materials at the site (Bolt, 1993).

The *Relative Earthquake Hazard Map of the Eugene-Springfield Metropolitan Area* is a composite hazard map depicting the relative hazard at any site due to the combination of the effects mentioned above. It delineates those areas that are likely to experience the most severe effects during a damaging earthquake. Areas of highest risk are those with high ground amplification, existing landslides, or steep slopes (>25° or >47%). Earthquake effects could range from people waking from their sleep to buildings collapsing.

Planners, lenders, insurers, and emergency responders can use such composite hazard maps for first-order hazard mitigation and response planning. It is very important to note that a relative hazard map predicts the tendency of a site to have greater or lesser damage than other sites in the area by assigning a range of zones. These zones, however, should not be used as the sole basis for any type of restrictive or exclusionary development policy.

HAZARD MAP METHODOLOGY

Geologic model

The most important element of any earthquake hazard evaluation is the development of a three-dimensional geologic model. For analysis of the amplification and liquefaction hazards, bedrock geology is not as important as the distribution and thickness of unconsolidated sediments. For analysis of the landslide hazard, bedrock geology of the steeper slopes (>25° or >47%) is important. For intermediate slopes (5°–25° or 9%–47%), the physical characteristics of the soil and colluvium covering the bedrock are of prime importance. The geologic model is developed from a combination of surface geologic mapping, surface shear-wave refraction, and subsurface borehole information. Surface geologic information for the Eugene-Springfield study was derived from a variety of sources, including published reports by Vokes and others (1951), Walker and Duncan (1989), Frank (1973), and Yeats and others (1991) and additional mapping, particularly of existing landslides, by author T.J. Wiley. Information on soil and colluvium was obtained from the Lane County soil survey (Patching, 1987). Authors Z. Wang and G.L. Black performed surface shear-wave refraction measurements.

The bedrock geology that makes up the hills in the southern, eastern, and northeastern portions of the Eugene-Springfield area is complex. However, the geology in that part of the study area relevant to the analysis of the amplification and liquefaction hazards (areas with slopes <5°, or <9%) is relatively simple. There, during the Pleistocene epoch (1.6-0.01 Ma), the Willamette and McKenzie Rivers cut deep channels into the underlying bedrock. These channels were filled with gravel. The geology in these areas tends to be two-tiered, but it varies slightly depending on whether an area is located inside or outside the modern (Holocene) meander belt of the Willamette and McKenzie Rivers. Inside the meander belt, thick Pleistocene gravels are covered with a thin veneer (~4.5 m or 15 ft) of Holocene gravel. Outside the Holocene meander belt, the same thick section of Pleistocene gravels is present, but it is covered instead by a thin veneer of silt. In the northern part of the study area, the silts were deposited by the latest Pleistocene Missoula floods, which entered the Willamette Valley in the Portland area about 12,000 years ago. In the southern part of the study area, these fine-grained deposits are mostly floodplain deposits derived from the major rivers and their tributaries.

The geology in the upland areas is more complex. There, lava flows and tuffaceous volcaniclastic rocks of the Western Cascades (Fisher Formation) interfinger with marine sedimentary rocks of the Coast Range (Spencer and Eugene Formations). Small intrusives further complicate the picture.

Information from surface geologic mapping and surface geophysical studies is integrated with subsurface data from a large borehole database to produce a three-dimensional geologic model. The boreholes used were originally drilled for water wells or foundation investigations. Water-well data were obtained from the Oregon Department of Water Resources (ODWR), which maintains a public database of all water wells drilled in the state. Information on boreholes drilled for foundation studies was obtained from consulting geotechnical engineers and used with permission. The resulting model defines the thickness of soil units beneath any location on the map so that their effect on earthquake damage can be assessed.

To assess the potential hazards associated with local geologic materials, data on more than just their thicknesses are needed. Additional geotechnical parameters include the Standard Penetration Test (SPT), which is a measure of the soil stiffness (relative density of a soil) and hence of its liquefaction potential. Many of the required measurements such as the SPT are acquired in the normal course of a foundation investigation. Thus, the needed information is available from many of the same sources as the thickness information.

In addition to the data acquired from borehole records, the assessment technique requires shear-wave velocities, which are used to determine the low-strain stiffness of the soils. Downhole measurements of shear-wave velocities were made at 15 sites in the Eugene-Springfield area. Of these 15 sites, the Oregon Department of Geology and Mineral Industries (DOGAMI) drilled 13, using conventional drilling techniques. In addition to shear-wave velocities measured in the boreholes, additional SPTs were performed and samples were obtained for grain-size analysis. At 12 additional sites, shear-wave velocities were determined with surface seismic methods. These sites also produced useful information on the thickness of geologic units. Seismic cone penetrometer measurements, a common method of obtaining shear-wave velocities, were not performed because of the pervasive occurrence of gravel in the study area.

All of this information is used to produce a detailed computer-generated map of the subsurface throughout the study area. Utilizing this information, the response to earthquake shaking at any specific location can be assessed.

HAZARD ANALYSIS

An earthquake causes damage through a variety of effects, including ground shaking, liquefaction, landslides, fault rupture, tsunamis, and seiches (Bolt, 1993). The severity of any one of these effects, or hazards, is influenced by a number of factors. Many of these factors can be assessed in relative terms without knowing the exact details of the earthquake itself.

The *Relative Earthquake Hazard Map* integrates three separate earthquake hazard components. They are (1) ground shaking amplification, (2) liquefaction, and (3) earthquake-induced landsliding. Fault rupture, tsunamis, and seiches are not considered to be threats in the Eugene-Springfield area. Each of these phenomena is a distinct and separate hazard and, in concert with others, can increase the severity of the total hazard at a given locality. The distinctions between components are important to technical specialists but less critical to a nontechnical audience. It therefore makes sense to generate a map of each of the individual hazard components that will be available to those able to use them and to then combine the individual maps into a simple, unified hazard map that generalizes the issues in a way useful to nonspecialists. A variety of raster- and vector-based GIS programs, including IDRISI (Eastman, 1997), MapInfo™, and Vertical Mapper™, were used to perform the map analysis.

Ground shaking amplification

The soils and soft sedimentary rocks near the surface can modify bedrock ground shaking caused by an earthquake. This modification can increase the strength of shaking (or alternatively decrease it) or change the frequency of the shaking. The nature of the modifications is determined by the thickness of the geologic materials and their physical properties, such as stiffness. Topography can also amplify shaking. Near the crests of bluffs, within a distance approximately equal to the height of the bluff, amplifications on the order of 1.5 times the bedrock shaking can occur (Ashford and Sitar, 1997). Because topographic effects are directional and not fully understood, they were not considered in this study.

Past DOGAMI earthquake hazard studies (Mabey and others, 1993, 1995a-d, 1996, 1997; Wang and Priest, 1995; and Wang and Leonard, 1996) used the sophisticated computer program SHAKE91 (Schnabel and others, 1972; Idriss and Sun, 1992) to estimate the effect of local geology on ground shaking. The SHAKE methodology has proven to be quite accurate in predicting the location and degree of ground shaking amplification in locations such as Mexico City and the San Francisco Bay area. However, most present-day amplification studies use a method first described by the Federal Emergency Management Agency (FEMA) (Building Seismic Safety Council, 1994) and adopted in the 1997 version of the Uniform Building Code (International Conference of Building Officials, 1997). This methodology will henceforth be referred to as the UBC–97 methodology. The SHAKE91 methodology is reserved for certain critical facilities (e.g., hospitals and fire and police stations) and sites underlain by very soft soils.

The UBC–97 methodology defines six soil categories based on average shear-wave velocity in the upper 30 m (100 ft) of the soil column. It then assigns amplification factors to each soil type. The six soil categories are hard rock (A), rock (B), very dense soil and soft rock (C), stiff soil profile (D), soft soil profile (E), and special soils (F). Category F soils are very soft soils requiring site-specific evaluation.

For the Eugene-Springfield area, the amplification hazard was analyzed using both the SHAKE91 and UBC–97 methodologies. The distribution of the amplification hazard from the SHAKE91 analysis was very similar to the result from the UBC–97 methodology. There were minor differences in the absolute value of the amplification hazard due to the fact that the UBC–97 method assigns a set amplification factor to soils that actually have a range of physical properties. The SHAKE91 methodology takes those subtle differences into account and also depends on input ground motions. The UBC–97 method was used to generate the amplification hazard map for this publication. This change (previous DOGAMI studies used the SHAKE91 method) was made because the UBC–97 method is (1) faster, (2) a more appropriate methodology for regional-scale maps, (3) compatible with current engineering design practice, and (4) independent of input ground motions.

Using the UBC–97 methodology, we defined three amplification hazard categories for the Eugene-Springfield area: (1) areas with amplification less than or equal to 1.0, (2) areas with amplification of 1.5, and (3) areas with amplification of 1.8.

The *Amplification Hazard Map* shown on the map sheet accompanying this report is the resulting three-category map of amplification hazard. The amplification hazard in the Eugene-Springfield area is not severe. Most of the study area does not amplify shaking; about 25% amplifies by a factor of 1.5; and only one small zone in the western part of the area, where there is a somewhat thicker sequence of unconsolidated fine-grained silt, amplifies by a factor of 1.8. What this means is that, if an earthquake produces bedrock accelerations of 0.2 g (where g is the acceleration due to gravity), a building that sits on a soil column that amplifies by a factor of 1.5 will experience accelerations of 0.3 g. The most recent study of the overall earthquake hazard in Oregon (Geomatrix Consultants, 1995) indicates that we can expect to experience bedrock accelerations in the Willamette Valley of about 0.25 *g* from local crustal earthquakes or from large subduction zone earthquakes. Accelerations of 0.25 *g* can cause slight damage in specially designed structures, considerable damage with partial collapse in ordinary substantial buildings, and great damage, often with total collapse, in poorly designed structures (Bolt, 1993).

Liquefaction

Liquefaction is a phenomenon in which shaking of a saturated soil causes its material properties to change so that it behaves as a liquid. In qualitative terms, the cause of liquefaction was described very well by Seed and Idriss (1982): "If a saturated sand is subjected to ground vibrations, it tends to compact and decrease in volume; if drainage is unable to occur, the tendency to decrease in volume results in an increase in pore water pressure, and if the pore water pressure builds up to the point at which it is equal to the overburden pressure, the effective stress becomes zero, the sand loses its strength completely, and it develops a liquefied state."

Soils that liquefy tend to be young, loose, granular soils that are saturated with water (National Research Council, 1985). Unsaturated soils will not liquefy, but they may settle. If an earthquake induces liquefaction, several things can happen. The liquefied layer and everything lying on top of it may move downslope; alternatively, it may oscillate with displacements large enough to rupture pipelines, move bridge abutments, or rupture building foundations. Light objects, such as underground storage tanks, can float toward the surface, and heavy objects, such as buildings, can sink. Typical displacements can range from centimeters to meters. Thus, if the soil at a site liquefies, the damage resulting from an earthquake can be significantly increased over what shaking alone might have caused.

Lateral spreading is a liquefaction-induced hazard that involves the displacement of essentially intact blocks of soil either downslope or toward a free face, such as a river channel. Movement occurs on a liquefied layer within the soil column. Lateral spreads generally develop on gentle slopes of <3° (5%) and can involve displacements of several meters (National Research Council, 1985).

Soils that are subject to liquefaction and/or lateral spreading can be identified. In the Eugene-Springfield area, there is a moderate lateral-spread hazard within the Holocene meander belts of the Willamette and McKenzie Rivers. Soils that liquefy tend to be young, unconsolidated, water-saturated, silts and sands with low clay content. Older (Pleistocene) gravels with a thin veneer of silt (outside the meander belt) or young (Holocene) sand and gravel (inside the meander belt) underlie that part of the Eugene-Springfield area potentially subject to liquefaction. Gravel will liquefy only under exceptional circumstances.

Shear-wave velocity is the best guide to the liquefaction potential of a gravel deposit. Very strong shaking can liquefy clean sands and gravels if their shear-wave velocities are less than about 215 m/s (705 ft/s) (Andrus and Stokoe, 1997). Shear-wave velocities measured in Pleistocene gravels by authors Z. Wang and G. Black are consistently greater than 300 m/s (984 ft/s), indicating that these gravels will not liquefy. Measured shear-wave velocities of Holocene sand and gravel typically range from 200 to 225 m/s (656–738 ft/s), indicating marginal potential for liquefaction and hence lateral spreading. The silts that overlie the gravel will not liquefy for three reasons: (1) They are water-saturated only under exceptional circumstances. (2) Their clay content is too high to permit liquefaction. (3) They are unconfined and too thin to permit the development of the excess pore water pressure required for liquefaction.

Within the modern meander belts of the Willamette and McKenzie Rivers, shear-wave velocity measurements indicate that the youngest sands and gravels may liquefy. This unit averages about 5 m (~16 ft) in thickness with a range of 0–8 m (0–26 ft). We assumed that sand and sandy gravel layers within this young geologic unit had the potential to undergo lateral-spread displacement. The displacement was calculated using the following empirical relationship from Bartlett and Youd (1995):

$$\log(D_H) = -15.787 + 1.178\,M - 0.927\log R - 0.013R + 0.429\log S + 0.348\log T_{15} + 4.527\log(100 - F_{15}) - 0.922D50_{15},$$

where D_H is the lateral-spread displacement in meters; M is the moment magnitude of the earthquake; R is the horizontal distance (in km) to the seismic energy source; S is the ground slope in percent; T_{15} is the cumulative thickness, in meters, of saturated cohesionless soils with $(N_1)_{60}$ values of ≤15; F_{15} is the average fines content in percent; and $D50_{15}$ is the mean grain size in millimeters.

The above calculation was performed within the Holocene meander belts for both design earthquakes, a M 8.5 at 100 km (62 mi) and a M 6.5 at 10 km (6 mi). Parameters used were slopes between 0° and 5° (0%–9%), cumulative thicknesses ranging from 0 to 3 m (0–10 ft), an average fines content of 10%, and a mean grain size of 0.1 mm (0.004 in) (equivalent to coarse sand). The displacements resulting from the M 8.5 earthquake at 100 km (62 mi) were approximately twice as large as those from the M 6.5 at 10 km (6 mi), and were used for the final hazard map. Calculated displacements ranged from 0 to 50 cm (0–20 in). We then assigned calculated displacements to a hazard category in such a way that displacements of 0–1 cm (0–0.4 in) were considered to represent no hazard, 1–10 cm (0.4–4 in) a low hazard, 10–100 cm (4–39 in) a moderate hazard, and displacements of >100 cm (39 in) a high hazard. Thus the lateral-spread hazard in the Eugene-Springfield area ranges from none to moderate. The result of the lateral-spread analysis is included as part of the slope instability map.

Slope instability (landslides)

In the Eugene-Springfield area, slope instability resulting from strong shaking will be a significant threat. The analysis for this study is based on state-of-practice dynamic analysis for slope stability and liquefaction. It also uses the empirical correlation of slope stability with engineering properties of materials, and the manipulation of data on local topography, engineering geology, and hydrology (Wang and others, 1998).

The particular method used to evaluate seismically induced ground deformation is a function of slope steepness. Different analytical techniques are used for different slope categories, because failure mechanisms vary depending on steepness. Slopes between 0° and 5° (0%–9%) fail by liquefaction and/or lateral spreading and are analyzed using the techniques discussed in the previous section. Steep slopes (>25°, or >47%) most commonly fail by rock falls, rock slides, and debris slides (Keefer, 1984) and are analyzed using empirical data that relate slope stability to degree of weathering, strength of cementation, spacing and openness of rock fractures, and hydrologic conditions. Moderate slopes produce larger numbers of rotational slumps and translational block slides in soil (Keefer, 1984). Therefore, slopes between 5° and 25° (9%–47%) are analyzed using a dynamic slope stability analysis that uses slope inclination, engineering-geologic characteristics of geologic units, and shaking parameters from design earthquakes as inputs.

These analyses are performed on computers using a variety of GIS programs. For the slope stability analyses a digital elevation model (DEM) is required. A DEM is nothing more than set of land elevations at regularly spaced intervals (like a grid) that blanket the study area, in this case the area enclosed by the Eugene-Springfield Metropolitan Plan Boundary. DEMs are produced by the U.S. Geological Survey (USGS) and have a grid spacing of 30 m (98 ft). We were fortunate in the Eugene-Springfield area to obtain DEMs produced especially for the Lane Council of Governments and the Cities of Eugene and Springfield. These DEMs have a cell spacing of about 9 m (30 ft). The GIS programs use the DEMs to calculate the slope angle at each point in the grid. This slope angle is one of the inputs into the stability analyses.

The grid spacing of the DEM is important because it determines the size of the smallest landslide that can be predicted. The 9-m (30-ft) grids used in this study are significantly better than the 30-m (98-ft) USGS grids. However, small landslides with dimensions of a few meters that occur in gullies and small hollows and may pose a relatively high risk will not show up on even a 9-m (30-ft) grid.

Slope analyses

Existing landslides

The movement characteristics of existing landslides are highly variable, ranging from active movement to stable. Although most earthquake-induced landslides occur in materials not previously involved in sliding (Keefer, 1984), it would require numerous site-specific studies to understand the nature of each of the landslides that currently exist in the Eugene-Springfield area. Therefore it was assumed that the slip planes of mapped landslides are at reduced shear strength of unknown value, and that the slide masses are inherently unstable under earthquake loading. Existing landslides are conservatively assigned to the highest hazard category. No analytical techniques were applied.

Steep slopes (>25° or >47%)

The analysis of the landslide potential on steep slopes is a three-step procedure. First, each bedrock outcrop in the study area was examined and evaluated for its failure potential. Then, based on the analysis of individual outcrops, the concentration of landslides in each geologic formation was calculated. Finally, each formation was placed into one of five slope instability hazard categories (None, Low, Moderate, High, Very High) based on landslide concentration.

Slopes >25° (>47%) are particularly vulnerable to bedrock failures. Keefer (1984, 1993) noted that more than 90% of earthquake-induced slope failures on rock slopes were rock falls and rock slides—typically thin, highly disrupted landslides that move at high velocities. The physical characteristics of the rock masses underlying steep slopes are of fundamental importance in evaluating their susceptibility to earthquake-induced slope failure. Accordingly, Robert Murray, a Registered Professional Geologist, examined a total of 213 outcrops, in order to evaluate their physical characteristics. This data set includes virtually all bedrock outcrops available for examination in the Eugene-Springfield study area. At each outcrop, the geologic unit, slope angle, degree of weathering, degree of induration, nature and spacing of fractures, and hydrologic conditions were noted. With this information, each outcrop was evaluated for failure potential, based on a decision tree (Figure 2) originally presented by Keefer (1993). Use of the decision tree results in the assignment of each outcrop to one of five failure susceptibility categories (Extremely High, Very High, High, Moderate, or Low).

Using the outcrop evaluations, the landslide concentration (number of landslides occurring per square kilometer, or LS/km^2) was calculated for each geolog-

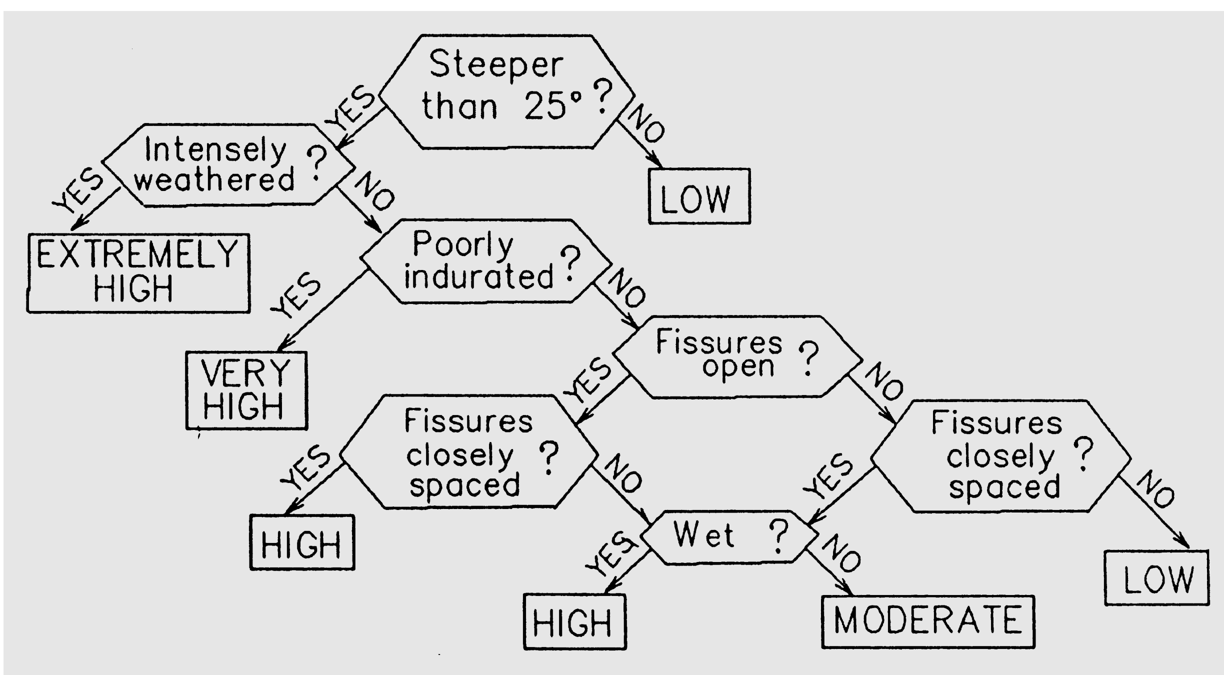

Figure 2. Decision tree for susceptibility of rock slopes to earthquake-induced landslides (from Keefer, 1993). For the Eugene-Springfield study, all slopes were assumed to be wet.

ic unit, using the following empirical relationship:

$$LS/\text{km}^2 = (32\ LS/\text{km}^2)(\%\ \text{extremely high}) + (8\ LS/\text{km}^2)(\%\ \text{very high}) + (2\ LS/\text{km}^2)(\%\ \text{high}) + (0.50\ LS/\text{km}^2)(\%\ \text{moderate}) + (0.125\ LS/\text{km}^2)(\%\ \text{low}),$$

where "% extremely high" represents the percentage of outcrops of a given geologic unit rated (by the decision tree) as having extremely high failure potential. The coefficient represents the average number of landslides per km^2 in study areas that (1) have experienced earthquake-induced landsliding and (2) have outcrop characteristics that indicate an extremely high failure potential. The other terms in the equation represent the other failure categories. The above equation is slightly modified from that presented in Keefer and Wang (1997) and Wang and others (1998) and was developed from data in Keefer (1993), relating landslide concentrations to earthquake magnitude and outcrop physical properties (as delineated in the decision tree).

Finally, based on the calculated landslide concentration, each geologic unit was placed into a slope instability hazard category. Landslide concentrations of >2 LS/km^2 were assigned to the high hazard category, those of 1–2 LS/km^2 were assigned to the moderate hazard category, and those of <1 LS/km^2 were assigned to the low hazard category. Table 1 lists the landslide concentrations and hazard category ratings for the geologic units occurring on steep slopes in the Eugene-Springfield area. More detailed discussions of the geologic units can be found in Keefer and Wang (1997) and Wang and others (1998).

Moderate slopes

The stability analysis for moderate slopes is based on the dynamic slope stability analysis of Newmark (1965) as verified and extended to regional-scale work by Wilson and Keefer (1983, 1985), Wieczorek and others (1985), Jibson (1993, 1996), and Jibson and Keefer (1993).

The process that assigns the soils that mantle moderate slopes to one of several slope-instability hazard categories takes several steps. First, using infinite slope analysis, the static factor of safety is calculated for each grid element with a slope between 5° and 25° (9%–47%). This factor of safety is then used to calculate the critical acceleration, which is the acceleration required to overcome friction and initiate sliding in the soil mass. The critical acceleration is used in conjunction with earthquake input parameters to calculate the total displacement that is expected to occur during the design earthquake. The total displacement is used to assign a slope-instability hazard category to each of these grid elements. Hazard categories used for the Eugene-Springfield study were (1) None—displacement <1 cm (0.4 in); (2) Low—displacement 1–10 cm (0.4–3.9 in); (3) Moderate—displacement 10–100 cm (3.9-39 in); (4) High—displacement >100 cm (>39 in); and (5) Existing—mapped landslides.

Factor-of-safety calculations depend on the thickness of the soil mass, the slope angle, the height of the water table, and physical characteristics of the soil mass. Physical characteristics include unit weight, cohesion, and angle of internal friction. For the Eugene-Springfield area, the soil survey of Lane County (Patching, 1987) was used to obtain information on the distribution of soil units and their physical properties. Physical characteristics include grain size distribution (soil classification), thickness and degree of saturation during the period December to April, plasticity indexes, and unit weights. Various sources were used to determine cohesion and angle of internal friction for the various soil units. These included NFEC (1986), Hammond and others (1992), Das (1994), and USDA (1994).

Many assumptions were involved in the factor-of-safety (FS) calculations:

Table 1. *Landslide concentrations and hazard categories for geologic units occurring in the Eugene-Springfield area*

Geologic unit	Formation	Rock type	LS/km^2	Hazard category
Tb		Non-Western-Cascade basalt	10.82	High
Te	Eugene	Marine sediments	5.34	High
Tf	Fisher	Volcaniclastic rocks	2.73	High
Ts	Spencer	Marine sediments	2.23	High
Tlb/Tuff	Little Butte	Welded tuff/dacite	2.00	High
Tcv	Little Butte	Cascade volcanic rocks	1.83	Moderate
Ti		Mafic intrusive rocks	1.30	Moderate

Failure: Failure is assumed to occur at the soil-bedrock interface during the period between December and April (the wettest months of the year).

Thickness: The soil survey (Patching, 1987) lists thicknesses for most soils. For some soils, however, the thickness is listed only as >60 in (152 cm). Based on conversations with Natural Resources Conservation Service personnel, the thickness for those soils was assumed to be 96 in (244 cm).

Density: Soil densities in Patching (1987) are tabulated as "moist bulk density" and listed as a range. USDA (1996) notes that "moist bulk density" is the density measured at "field" moisture content. Because most field work is done in the summer, when the soils are thoroughly dried, it was assumed that the dry bulk density for FS calculations was the average of the "moist bulk density" range given in Patching (1987). Because it is assumed that the earthquake occurs during a wet period, the unit weights used in the FS calculations assume 90% saturation.

Cohesion: DOGAMI ran consolidated, undrained triaxial shear tests on two Shelby tube samples from a single location. Cohesion measured in the two samples was 2.78 kPa (58 lb/ft^2) and 4.78 kPa (100 lb/ft^2). Trial FS calculations resulted in factors of safety of <1 for many obviously stable slopes, when zero cohesion was assumed. Therefore, the following assumptions regarding cohesion were made: (1) For sandy and gravelly soils with low clay contents, cohesion = 0. (2) If the minimum clay content was <35%, cohesion was assumed to be 2.78 kPa (58 lb/ft^2). (3) If the minimum clay content was between 35% and 60%, cohesion was assumed to be 3.78 kPa (79 lb/ft^2). (4) If the minimum clay content was >60%, cohesion was assumed to be 4.78 kPa (100 lb/ft^2). Neither the extra strength provided by tree roots nor the tree surcharge was considered in the analysis.

Water table: If the soil survey (Patching, 1987) described the soil as well drained, the water table was assumed to be below the soil-bedrock contact. If the depth to the water table for the period December-April was given as 1–2 ft (0.3–0.6 m), it was assumed to be 1 ft (0.3 m). If the depth to the water table for the period December-April was given as 0–1 ft (0–0.3 m), it was assumed to be at the surface.

FS calculations were performed in Microsoft Excel™ spreadsheet for slopes between 5° and 25° (9%–47%).

Once the factor of safety for any slope element is known, it is possible to calculate the critical acceleration a_c (Newmark, 1965). The critical acceleration is the acceleration required to overcome frictional resistance and initiate sliding. It is calculated from the following equation (Newmark, 1965):

$$a_c = (FS - 1)g \sin(\alpha),$$

where a_c is the critical acceleration in terms of acceleration due to gravity, g, FS is the factor of safety, g is the acceleration due to gravity (equal to one in this equation), and α is the angle from the horizontal by which the center of the mass of the potential landslide block first moves. For a translational slide, assuming that the ground surface is parallel to the failure surface, a is the slope angle.

Once the critical acceleration is known, earthquakes can be used to predict the amount of expected displacement for any input ground motion. Two design earthquakes were utilized in the Eugene-Springfield study. The first was a M 8.5 subduction zone earthquake at a distance of 100 km (62 mi). The second was a M 6.5 event at a distance of 10 km (6.2 mi). In a classic Newmark (1965) analysis, complete time histories of the earthquakes at specific locations are examined, and, for intervals in the time history where the acceleration exceeds the critical acceleration, the record is integrated twice to produce a record of displacement vs. time. However, a modified form of that technique was used in the Eugene-Springfield study. Arias (1970) developed a relatively simple method of expressing the severity of strong ground shaking, known as the Arias intensity. The Arias intensity (I_a) is the integration over time of the acceleration squared and has units of velocity. Wilson and Keefer (1985) developed an empirical equation that relates Arias intensity to earthquake magnitude and distance to the earthquake source:

$$\log(I_a) = M - 2 \log R - 4.1,$$

where I_a is the Arias intensity, M is the earthquake moment magnitude, and R is the earthquake source distance in kilometers.

Note that the Arias intensity for a M 8.5 earthquake at 100 km (62 mi) is identical to the Arias intensity of a M 6.5 earthquake at 10 km (6.2 mi).

Jibson (1993) and Jibson and Keefer (1993) developed empirical relationships between Newmark displacement (D_N, in cm), critical acceleration (a_c), and Arias intensity (I_a):

$$\log(D_N) = 1.460\log(I_a) - 6.642(a_c) + 1.546$$

This equation was used to determine the expected slope displacement for each grid point where the slope is between 5° (9%) and 25° (47%). Finally, each element of the slope grid was assigned to a hazard category (None, Low, Moderate, High) based on the calculated Newmark displacements.

In practical (GIS) terms, the procedure is time consuming but relatively simple. All calculations (factor of safety, Arias intensity, critical acceleration, Newmark displacement) are performed in a Microsoft Excel™ spreadsheet. In addition, there are two digital files. One contains the soil map for the Eugene-Springfield study area. The second is the slope map (calculated from the DEM) on a 30-ft (9-m) grid spacing within the study area. Using MapInfo™, the location of each slope grid point is mapped within the soil map. A series of queries is used to assign hazard categories. For instance, soil type 45C (Patching, 1987) has a calculated Newmark displacement of between 10 cm (3.9 in) and 100 cm (39 in) on slopes of 19°–25° (34%–47%). The GIS files are queried to find all points where soil type 45C occurs on slopes of 19°–25° (34%–47%). The resulting points are assigned to hazard category 3 (Moderate).

Digital files from the three methodologies are combined to produce the final slope instability hazard map.

RELATIVE EARTHQUAKE HAZARD MAP

The *Relative Earthquake Hazard Map of the Eugene-Springfield Metropolitan Area* was created to show which areas will have the greatest tendency to experience damage due to any one hazard or a combination of hazards. Hazard maps were generated for two individual hazards, ground motion amplification and slope instability. For the purpose of creating the final relative hazard map, the individual map categories were assigned to zones 0, 1, 2, or 3, with 3 being the greatest hazard. For the ground motion amplification map, amplification of ≤1 was assigned to zone 1, 1.5 was assigned to zone 2, and 1.8 was assigned to zone 3. For the slope instability map, the "None" category was assigned to zone 0, the "Low" category to zone 1, the "Moderate" category to zone 2, and the "High" and "Existing" categories to zone 3. For every point (using a 30-m cell spacing) on the map, the zone rating for each individual hazard (amplification and slope instability) was squared, and the resulting numbers were added together. Then the square root of this sum was taken and rounded to the nearest whole number. A result of 4 was assigned to category A, 3 to category B, 2 to category C, and 1 to category D. While the production of the individual hazard maps is different from previous DOGAMI relative earthquake hazard studies (Wang and Priest, 1995; Wang and Leonard, 1996; Mabey and others, 1997, Madin and Wang, 1999, 2000a-c), the method of production of the final relative hazard map is identical. Thus relative hazard maps produced for the Eugene-Springfield area are directly comparable to similar studies in the Siletz Bay area, Portland, Salem, and 28 other urban areas in western Oregon.

Note that no Zone A hazard zones occur in the Eugene-Springfield area. The way the rating system is designed, areas with a high hazard from a single local effect or areas with a combination of lesser single ratings are assigned to Zone B, the second highest hazard category. Zone A ratings occur as a result of two or more high ratings of local effects. The Zone B category should not be underrated, since it can result from a single very severe hazard.

USE OF THE RELATIVE EARTHQUAKE HAZARD MAP

The *Relative Earthquake Hazard Map of the Eugene-Springfield Metropolitan Area* delineates those areas where earthquakes present, on average, the greatest hazard. This information can be used to develop a variety of hazard mitigation policies, most of which were mentioned in the introduction. This information, however, should be carefully considered and understood, so that inappropriate use is avoided.

Emergency response and hazard mitigation

One of the key uses of this map is to develop emergency response plans. The areas indicated as having higher hazard would be the areas where the greatest and most abundant damage will tend to occur. Efforts and funds for both urban renewal and strengthening or replacing older and weaker buildings can be focused on the areas where the effects of earthquakes will be the greatest. The location of future urban expansion or intensified development should consider earthquake hazards.

Requirements placed on development could be based on the hazard zone in which the development is located. For example, the type of site-specific earthquake hazard investigation that is required could be based on the hazard zone. When the relative earthquake hazard maps are incorporated into ArcInfo-based GIS programs of the Lane Council of Governments, they can easily be combined with any of the other land use or hazard information in that system.

Lifelines

Lifelines include road and access systems, including railroads, airports and runways, bridges, and over- and underpasses; as well as utilities and distribution systems. The *Relative Earthquake Hazard Map* and its component single-hazard maps are especially useful for expected damage estimation and mitigation for lifelines. The distributed character of lifelines precludes comprehensive site-specific evaluations. These hazard maps allow quantitative estimates of the hazard throughout a lifeline system. This information can be used for assessing vulnerability as well as indicating priorities and approaches for mitigation.

Engineering

The specific quantitative values of any single hazard that were calculated for this map are not a substitute for site-specific evaluations based on subsurface information gathered at a site. The calculated values may, however, be used to good purpose in the absence of such site-specific information, e.g., at the feasibility-study or preliminary-design stage. In most cases, the quantitative values calculated for these maps would be superior to a qualitative estimate based solely on lithology or non-site-specific information. Any significant deviation of observed site geology from the geologic model used in the analyses indicates the need for additional analyses at the site.

Relative hazard

It is important to recognize the limitations of the *Relative Earthquake Hazard Map*, which in no way includes information regarding the probability of earthquake damage occurring. Rather, it shows that when shaking occurs, the damage is more likely to occur, or to be more severe, in the higher hazard areas. The exact probability that such shaking would occur is yet to be determined.

Neither should the higher hazard areas be viewed as unsafe. Except for landslides, the earthquake effects that are factored into the *Relative Earthquake Hazard Map* are not life threatening in and of themselves. What is life threatening is the way that structures such as buildings and bridges respond to these effects. Locations are not necessarily unsafe or even less safe, but the structures there may be.

The map depicts trends and tendencies. In all cases, the actual threat at a given location can be assessed only by some degree of site-specific assessment. This is similar to being able to say, demographically, that a zip code zone contains an economic middle class, but within that zone there easily could be individuals or neighborhoods significantly richer or poorer.

In summary, some parts of the Eugene-Springfield area are more prone to earthquake effects than others. These maps provide one way this fact can be taken into account in planning, development, and decision-making.

ACKNOWLEDGMENTS

Robert Murray, Registered Professional Geologist, examined all outcrops in the Eugene-Springfield area to determine their susceptibility to failure on steep slopes.

An Advisory Committee composed of members of the public, local business, the professional community, and local government provided valuable input and direction for the project. Committee members included Tom Buckhouse (Eugene Water and Electric Board), Bill Clingman (Lane Council of Governments), John Goodsen (Lane County Public Works), Dennis Hellesvig (City of Eugene), Ike Jensen (Lane County Emergency Management), Richard Maris (Berry Architects), Tom Miller (Department of Civil Engineering, Oregon State University), Emile Mortier (Mortier Engineering), Randy Prince (Citizen), Dave Puent (City of Springfield), and Christine Theodoropoulos (Department of Architecture, University of Oregon).

Excellent reviews of the final maps and text were provided by Kenneth Cruikshank (Department of Geology, Portland State University), Stephen Dickenson (Department of Civil, Construction and Environmental Engineering, Oregon State University), and Matthew Mabey (Department of Geology, Brigham Young University).

Thank you all!

REFERENCES CITED

Andrus, R.D., and Stokoe, K.H., 1997, Liquefaction resistance based on shear wave velocity: Report to the NCEER Workshop on Evaluation of Liquefaction Resistance (9/18/97 Version), Jan. 4–5, Salt Lake City, Utah.

Arias, A., 1970, A measure of earthquake intensity, in Hansen, R.J., ed., Seismic design for nuclear power plants: Cambridge, Mass., Massachusetts Institute of Technology Press, p. 438–483.

Ashford, S.A., and Sitar, N., 1997, Topographic effects on the seismic response of steep slopes: Seismological Society of America Bulletin, v. 87, no. 3, p. 701–709.

Atwater, B.F., 1987, Evidence for great Holocene earthquakes along the outer coast of Washington State: Science, v. 236, p. 942–944.

Atwater, B.F., and Hemphill-Haley, E., 1997, Recurrence intervals for great earthquakes of the past 3,500 years at northeastern Willapa Bay, Washington: U.S. Geological Survey Professional Paper 1576, 108 p.

Bartlett, S.F., and Youd, T.L., 1995, Empirical prediction of liquefaction-induced lateral spread: Journal of Geotechnical Engineering, v. 121, no. 4, p. 316–329.

Bolt, B.A., 1993, Earthquakes: New York, W.H. Freeman and Co., 331 p.

Building Seismic Safety Council, 1994, NEHRP recommended provisions for seismic regulations for new buildings, 1994 edition, Part 1: Provisions: Federal Emergency Management Agency Publication FEMA 222A / May 1995, 290 p.

Das, B.M., 1994, Principles of geotechnical engineering: Boston, Mass., PWS Publishing Company, 672 p.

Eastmann, J.R., 1997, IDRISI for Windows Geographic Analysis System. User's guide, version 2.0, January 1997, revision 5, December 1997: Worcester, Mass., Clark University, Clark Labs for Cartographic Technology and Geographic Analysis, var. pag.

Frank, F.J., 1973, Ground water in the Eugene-Springfield area, southern Willamette Valley, Oregon: U.S. Geological Survey Water-Supply Paper 2018, 65 p.

Geomatrix Consultants, Inc., 1995, Seismic design mapping, State of Oregon: Final report to Oregon Department of Transportation, Project no. 2442, var. pag.

Hammond, C., Hall, D., Miller, S., and Swetik, P., 1992, Level I Stability Analysis (LISA), documentation for version 2.0: U.S.D.A. Forest Service, Intermountain Research Station, General Technical Report INT–285, 190 p.

Heaton, T.H., and Hartzell, S.H., 1987, Earthquake hazards on the Cascadia subduction zone: Science, v. 236, p. 162-168.

Idriss, I.M., and Sun, J.I., 1992, User's manual for SHAKE91, a computer program for conducting equivalent linear seismic response analyses of horizontally layered soil deposits: Davis, Calif., University of California at Davis, Department of Civil and Environmental Engineering, Center for Geotechnical Modeling, var. pag.

International Conference of Building Officials, 1997, 1997 Uniform building code, v. 2, Structural engineering design provisions: International Conference of Building Officials, 492 p.

Jibson, R.W., 1993, Predicting earthquake-induced landslide displacements using Newmark's sliding block analysis: Washington, D.C., National Research Council Transportation Research Record 1411, p. 9–17.

Jibson, R.W., 1996, Use of landslides for paleoseismic analysis: Engineering Geology, v. 43, p. 291–323.

Jibson, R.W., and Keefer, D.K., 1993, Analysis of the seismic origin of landslides: Examples from the New Madrid seismic zone: Geological Society of America Bulletin, v. 105, no. 4, p. 521–536.

Kanamori, H., 1977, The energy release in great earthquakes: Journal of Geophysical Research, v. 82, p. 2981–2987.

Keefer, D.K., 1984, Landslides caused by earthquakes: Geological Society of America Bulletin, v. 95, no. 4, p. 406–421.

Keefer, D.K., 1993, The susceptibility of rock slopes to earthquake-induced failure: Association of Engineering Geologists Bulletin, v. 30, no. 3, p. 353–361.

Keefer, D.K., and Wang, Y., 1997, A method for predicting slope instability for earthquake hazard maps: Preliminary report, *in* Wang, Y. and Neuendorf, K.K.E., eds., Earthquakes—Converging at Cascadia. Symposium proceedings: Association of Engineering Geologists Special Publication 10/ Oregon Department of Geology and Mineral Industries Special Paper 28, p. 39–52.

Levson, V.M., Monahan, P.A., Meldrum, D.G., Matysek, P.F., Gerath, R.F., Watts, B.D., Sy, A., and Yan, L., 1995, Surficial geology and earthquake hazard mapping, Chilliwack, British Columbia (92G/1 and H/4), *in* Grant, B.M., and Newell, J.M., eds., Geological Fieldwork 1995: British Columbia Ministry of Energy, Mines, and Petroleum Resources Paper 1996–1, p.191–203

Mabey, M.A., Black, G.L., Madin, I.P., Meier, D.B., Youd, T.L., Jones, C.F., and Rice, J.B., 1997, Relative earthquake hazard map of the Portland metro region, Clackamas, Multnomah, and Washington Counties, Oregon: Oregon Department of Geology and Mineral Industries Interpretive Map Series IMS–1, scale 1:62,500.

Mabey, M.A., Madin, I.P., Black, G.L., and Meier, D.B., 1996, Relative earthquake hazard map of the Linnton quadrangle, Multnomah and Washington Counties, Oregon: Oregon Department of Geology and Mineral Industries Geological Map Series GMS–104, scales 1:24,000 and 1:55,000.

Mabey, M.A., Madin, I.P., and Meier, D.B., 1995a, Relative earthquake hazard map of the Beaverton quadrangle, Washington County: Oregon Department of Geology and Mineral Industries Geological Map Series GMS–90, scale 1:24,000.

———1995b, Relative earthquake hazard map of the Gladstone quadrangle, Clackamas and Multnomah Counties: Oregon Department of Geology and Mineral Industries Geological Map Series GMS–92, scale 1:24,000.

———1995c, Relative earthquake hazard map of the Lake Oswego quadrangle, Clackamas, Multnomah and Washington Counties: Oregon Department of Geology and Mineral Industries Geological Map Series GMS–91, scale 1:24,000.

Mabey, M.A., Madin, I.P., Meier, D.B., and Palmer, S.P., 1995d, Relative earthquake hazard map of the Mount Tabor quadrangle, Multnomah County, Oregon, and Clark County, Washington: Oregon Department of Geology and Mineral Industries Geological Map Series GMS–89, scale 1:24,000.

Mabey, M.A., Madin, I.P., Youd, T.L., and Jones, C.F., 1993, Earthquake hazard maps of the Portland quadrangle, Multnomah and Washington Counties, Oregon, and Clark County, Washington: Oregon Department of Geology and Mineral Industries Geological Map Series GMS-79, 106 p., scale 1:24,000

Madin, I.P., Priest, G.R., Mabey, M.A., Malone, S., Yelin, T.S., and Meier, D., 1993, March 25, 1993, Scotts Mills earthquake—western Oregon's wake-up call: Oregon Geology, v. 55, no. 3, p. 51–57.

Madin, I.P. and Wang, Z., 1999, Relative earthquake hazard maps for selected urban areas in western Oregon: Astoria-Warrenton, Brookings, Coquille, Florence-Dunes City, Lincoln City, Newport, Reedsport-Winchester Bay, Seaside-Gearhart-Cannon Beach, Tillamook: Oregon Department of Geology and Mineral Industries Interpretive Map Series IMS–10, 25 p., 2 map sheets, scale 1:24,000.

———2000a, Relative earthquake hazard maps for selected urban areas in western Oregon: Dallas, Hood River, McMinnville-Dayton-Lafayette, Monmouth-Independence, Newberg-Dundee, Sandy, Sheridan-Willamina, St. Helens-Columbia City-Scappoose: Oregon Department of Geology and Mineral Industries Interpretive Map Series IMS–7, 24 p., 2 map sheets, scale 1:24,000.

———2000b, Relative earthquake hazard maps for selected urban areas in western Oregon: Canby-Barlow-Aurora, Lebanon, Silverton-Mount Angel, Stayton-Sublimity-Aumsville, Sweet Home, Woodburn-Hubbard: Oregon Department of Geology and Mineral Industries Interpretive Map Series IMS–8, 22 p., 1 map sheet, scale 1:24,000.

———2000c, Relative earthquake hazard maps for selected urban areas in western Oregon: Ashland, Cottage Grove, Grants Pass, Roseburg, Sutherlin-Oakland: Oregon Department of Geology and Mineral Industries Interpretive Map Series IMS–9, 21 p., 1 map sheet, scale 1:24,000.

National Research Council, Commission on Engineering and Technical Systems, Committee on Earthquake Engineering, 1985, Liquefaction of soils during earthquakes: Washington, D.C., National Academy Press, 240 p.Naval Facilities Engineering Command (NFEC), 1986, Soil mechanics: Alexandria, Va., Naval Facilities Engineering Command, 347 p.

Newmark, N.M., 1965, Effects of earthquakes on dams and embankments: Géotechnique, v. 15, no. 2, p. 139–159.

Patching, W.R., 1987, Soil survey of Lane County, Oregon: USDA Natural Resources Conservation Service, 369 p.

Schnabel, P.B., Lysmer, J., and Seed, H.B., 1972, SHAKE—A computer program for earthquake response analysis of horizontally layered sites: Berkeley, Calif., University of California, Earthquake Engineering Research Center Report UBC/EERC–72–12, 102 p.

Seed, H.B., and Idriss, 1982, Ground motions and soil liquefaction during earthquakes: Earthquake Engineering Institute Monograph, 134 p.

U.S. Department of Agriculture (USDA), 1994, Slope stability reference guide for national forests in the United States, volume I: Washington, D.C., USDA Forest Service Engineering Staff Report EM-7170-13.

———1996, Soil Survey Laboratory Methods Manual: USDA Natural Resources Conservation Service Soil Survey Investigations Report 42, Version 3.0, 693 p.

Vokes, H.E., Snavely, P.D., and Myers, D.A., 1951, Geology of the southern and southwestern border areas of the Willamette Valley, Oregon: U.S. Geological Survey Oil and Gas Investigations Map OM–110, scale 1:62,500.

Walker, G.W., and Duncan, R.S., 1989, Geologic map of the Salem 1° by 2° quadrangle, western Oregon: U.S. Geological Survey Miscellaneous Investigations Series Map I–1893, scale 1:250,000.

Wang, Y., Keefer, D.K., and Wang, Z., 1998, Seismic hazard mapping in Eugene-Springfield, Oregon: Oregon Geology, v. 60, no. 2, p. 31-41.

Wang, Y., and Leonard, W.J., 1996, Relative earthquake hazard maps of the Salem East and Salem West quadrangles, Marion and Polk Counties, Oregon: Oregon Department of Geology and Mineral Industries Geological Map Series GMS–105, scale 1:24,000.

Wang, Y., and Priest, G.R., 1995, Relative earthquake hazard maps of the Siletz Bay area, coastal Lincoln County, Oregon: Oregon Department of Geology and Mineral Industries Geological Map Series GMS–93, scales 1:12,000 and 1:24,000.

Weaver, C.S., and Shedlock, K.M., 1989, Potential subduction, probable intraplate, and known crustal earthquake source areas in the Cascadia subduction zone, *in* Hayes, W.W., ed., 3rd Annual Workshop on "Earthquake Hazards in the Puget Sound, Portland Area," Proceedings of Conference XLVIII: U.S. Geological Survey Open-File Report 89–465, p. 11–26.

Wieczorek, G.F., Wilson, R.C., and Harp, E.L., 1985, Map showing slope stability during earthquakes in San Mateo County, California: U.S. Geological Survey Miscellaneous Investigations Series Map I–1257–E, scale 1:62,500.

Wiley, T.J., Sherrod, D.R., Keefer, D.K., Qamar, A., Schuster, R.L., Dewey, J.W., Mabey, M.A., Black, G.L., and Wells, R.E., 1993, Klamath Falls earthquakes, September 20, 1993—including the strongest quake ever measured in Oregon: Oregon Geology, v. 55, no. 6, p. 127–134.

Wilson, R.C., and Keefer, D.K., 1983, Dynamic analysis of a slope failure from the August 6, 1979, Coyote Lake, California, earthquake: Seismological Society of America Bulletin, v. 73, no.3, p. 863–877.

———1985, Predicting areal limits of earthquake-induced landsliding, *in* Ziony, J.L., ed., Evaluating earthquake hazards in the Los Angeles region; an earth-science perspective: U.S. Geological Survey Professional Paper 1360, p. 316–345.

Yeats, R.S., Graven, E.P., Werner, K.S., Goldfinger, C., and Popowski, T.A., 1991, Tectonics of the Willamette Valley, Oregon: U.S. Geological Survey Open-File Report 91–441–P, 47 p.

Yelin, T.S., Tarr, A.C., Michael, J.A., and Weaver, C.S., 1994, Washington and Oregon earthquake history and hazards: U.S. Geological Survey Open-File Report 94–226–B, 11 p.